Squeeze Film Damping Effect on the Dynamic Response of a MEMS Torsion Mirror

Feixia Pan*, Joel Kubby*, Eric Peeters*, Alex T. Tran*, Subrata Mukherjee**
* Xerox Wilson Research Center, 800 Phillips Road, Webster, NY 14580
** Department of Applied Mechanics, Cornell University, Ithaca, NY 14850

ABSTRACT

Analytical formulae for the squeeze film damping torque on a MEMS torsion mirror are derived based on series solutions to the linearized Reynold's equation. The derivation is carried out under the assumption that the angular displacement of the mirror is small and is a harmonic function of time. This analytical squeeze film damping model is verified by numerically solving the nonlinear isothermal Reynold's equation [1], and by conducting experimental measurements on a prototype device. Finally it is shown that although the analytical damping model is derived under the assumption of harmonic time response of the torsion mirror, it is still valid for the case of non-harmonic response, as long as the squeeze number is fairly small.

Keywords: Squeeze film damping torque, torsion mirror, Reynold's equation, series solutions.

INTRODUCTION

In our torsion mirror design [2], the dynamic motion of a mirror under certain excitation conditions must be predicted. An important issue involved in this prediction is to determine the squeeze film damping effect due to the motion of the air in the gap between a movable mirror and a fixed substrate.

Because of its wide technological applications, the squeeze film damping behavior has been extensively studied in such areas as gas film lubrication [3], accelerometer [4,5,6,7] and control system design. However, most of the previous researches are concerned with the squeeze film damping due to the harmonic normal motion of two parallel or substantially parallel surfaces. There have only been a few investigations on the squeeze film damping torque generated during the relative rotation of two very closely spaced surfaces [8,9,10].

In this presentation, we first review the nonlinear isothermal Reynold's equation for the squeeze film damping analysis, then linearize this equation, and derive series solutions to the linearized system. Analytical formulae for the damping torque are thus developed and are used to predict the dynamic response of a mirror which has been fabricated as a prototype device . This analytical damping model is verified by comparing it with the numerical damping model, and further verified by experimental measurements. Finally we discuss characteristics of the squeeze film damping under the condition of small squeeze number, and address issues on the application of the analytical damping model.

REYNOLD'S EQUATION

Figure 1 shows a schematic diagram of the rotation of a MEMS torsion mirror.

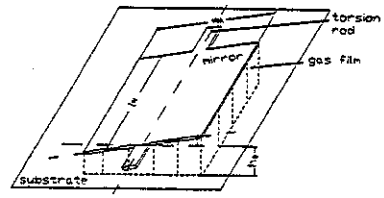

Figure 1. schematic diagram of a MEMS mirror.

As the mirror rotates about the torsion rods, it is subjected to squeeze film damping from the air that is squeezed underneath the mirror, in the small gap between the reflecting mirror surface and the substrate. The squeeze film damping torque results from the pressure variation over the mirror surface. The equation governing the pressure distribution in the squeeze film is the nonlinear isothermal Reynold's equation [1]:

$$\frac{\partial}{\partial X}\left(H^3 P\frac{\partial P}{\partial X}\right)+\frac{\partial}{\partial Y}\left(H^3 P\frac{\partial P}{\partial Y}\right)=\sigma\frac{\partial(PH)}{\partial T}, \qquad (1)$$

where P is the normalized pressure, $P=\frac{p}{p_a}$, with p_a being the ambient pressure, X and Y denote the normalized spatial coordinates, $X=\frac{x}{l_M}, Y=\frac{y}{l_M}$, with l_M being the mirror length, H is the normalized squeeze film thickness, $H=\frac{h}{h_0}$, with h_0 being the

initial squeeze film thickness, h_0 is the squeeze number, $\sigma = \frac{12\mu\omega {l_M}^2}{p_a {h_0}^2}$, μ is the air viscosity, ω is a typical frequency of the squeeze components, and T is a scaled time, $T = \omega t$.

In general, the squeeze film damping effect includes the air spring effect and the dissipative damping effect. It has been pointed out by Langlois [1] and Starr [5] that for small values of σ, the film behaves as though the fluids were incompressible, while for very large value of σ, the film essentially acts as an air spring and exhibits little dissipation. In our design, for any frequency ω below or around the first natural frequency of the mirror, σ is a very small quantity, and thus the dissipative damping force should be dominant. At first, however, we consider both the dissipative damping force and the air spring force. We then find that the air spring effect is very small and thus is negligible.

ANALYTICAL DAMPING MODEL

To perform analytical modeling analysis, we first simplify the nonlinear isothermal Reynold's equation (1) by assuming that the motion of the mirror is small and thus the pressure variation in the squeeze film relative to the ambient is also small. Upon introducing a small perturbation parameter δ such that

$$H = 1 + \delta H_1, \quad P = 1 + \delta \Pi, \tag{2}$$

we obtain a linearized Reynold's equation [7,10]:

$$\frac{\partial^2 \Pi}{\partial X^2} + \frac{\partial^2 \Pi}{\partial Y^2} = \sigma\left(\frac{\partial \Pi}{\partial T} + \frac{\partial H_1}{\partial T}\right). \tag{3}$$

The boundary conditions associated with (3) are given by:

$$\Pi\left(\pm\frac{1}{2}, Y, T\right) = \Pi\left(X, \pm\frac{b}{2}, T\right) = 0, \tag{4}$$

where $b = \frac{w_M}{l_M}$, and w_M is the mirror width. With the mirror approximated as a rigid body, the relationship between the normalized squeeze film thickness H and the mirror angular displacement θ becomes

$$H = \frac{h}{h_0} = 1 + \frac{y\theta}{h_0} = 1 + Y\frac{l_M}{h_0}\theta. \tag{5}$$

To derive analytical formulae for the squeeze film damping from (3) and (4), we first assume that the angular displacement of the mirror is a harmonic function of time. We will return to this and point out that this assumption is very restrictive and is in fact unnecessary.

Under the assumption of harmonic response, the boundary value problem constituted by (3) and (4) becomes:

$$\frac{\partial^2 \Phi}{\partial X^2} + \frac{\partial^2 \Phi}{\partial Y^2} - i\sigma\Phi = i\sigma Y, \tag{6}$$

$$\Phi\left(\pm\frac{1}{2}, Y\right) = \Phi\left(X, \pm\frac{b}{2}\right) = 0. \tag{7}$$

where we define $\Phi(X,Y)$ as a complex variable

$$\Phi(X,Y) \equiv \Pi_1(X,Y) + i\Pi_2(X,Y), \tag{8}$$

for which

$$\Delta P = \delta\Pi = \frac{l_M\Theta}{h_0}\Pi = \frac{l_M}{h_0}\left(\Pi_1\theta + \Pi_2\frac{1}{\omega}\dot{\theta}\right), \tag{9}$$

with Θ being the amplitude of the harmonic angular displacement. The perturbation parameter $\delta = \frac{l_M\Theta}{h_0}$ will be a small quantity so long as Θ is small, which it is in our mirror design ($\Theta \le \pm 1^0$). We next derive the series solutions for the above boundary value problem.

Fourier Series Solution

In accordance with the boundary condition (7), we assume

$$\Phi(X,Y) = \sum_{n=1}^{\infty} f_n(X)\sin\frac{2n\pi Y}{b}. \tag{10}$$

Substituting (10) into (6) and recalling (8), we obtain

$$\Pi_1 = \sum_{n=1}^{\infty}\left(\begin{matrix}C_{1n}\cos r_{2n}X\cosh r_{1n}X - \\ C_{2n}\sin r_{2n}X\sinh r_{1n}X - C_{3n}\end{matrix}\right)\sin\frac{2n\pi Y}{b},$$
$$\Pi_2 = \sum_{n=1}^{\infty}\left(\begin{matrix}C_{2n}\cos r_{2n}X\cosh r_{1n}X + \\ C_{1n}\sin r_{2n}X\sinh r_{1n}X - C_{4n}\end{matrix}\right)\sin\frac{2n\pi Y}{b}. \tag{11}$$

Based on (9) and (11), the damping torque is determined by integrating the contribution of the pressure variation over the mirror surface:

$$T_d = \frac{{l_M}^2 {w_M}^2 p_a}{2\pi h_0}\left(\theta\sum_{n=1}^{\infty}C_{9n} + \frac{1}{\omega}\dot{\theta}\sum_{n=1}^{\infty}C_{10n}\right), \tag{12}$$

where we define [11]:

$$C_{9n} \equiv \frac{\sigma b}{\Delta_1 n^2 \pi}\left[\sigma C_{7n} - \left(\frac{2n\pi}{b}\right)^2 C_{8n}\right],$$

$$C_{10n} \equiv \frac{\sigma b}{\Delta_1 n^2 \pi}\left[\left(\frac{2n\pi}{b}\right)^2 C_{7n} + \sigma C_{8n}\right],$$

$$C_{7n} \equiv \frac{r_{1n}\sinh r_{1n} + r_{2n}\sin r_{2n}}{\Delta_2 (r_{1n}^2 + r_{2n}^2)} - 1,$$

$$C_{8n} \equiv \frac{-r_{2n}\sinh r_{1n} + r_{1n}\sin r_{2n}}{\Delta_2 (r_{1n}^2 + r_{2n}^2)}, \qquad (13)$$

$$r_{1n}, r_{2n} \equiv \sqrt{\frac{1}{2}\left[\pm\left(\frac{2n\pi}{b}\right)^2 + \sqrt{\Delta_1}\right]},$$

$$\Delta_1 \equiv \left(\frac{2n\pi}{b}\right)^4 + \sigma^2, \Delta_2 \equiv \cos^2\frac{r_{2n}}{2} + \sinh^2\frac{r_{1n}}{2}.$$

Double Sine Series Solution

We assume

$$\Phi(X,Y) = \sum_{m=1}^{\infty}\sum_{n=1}^{\infty} C_{mn}\sin m\pi\left(X+\frac{1}{2}\right)\sin\frac{n\pi}{b}\left(Y+\frac{b}{2}\right), \qquad (14)$$

to satisfy the boundary condition (7). The coefficients C_{mn} are determined by substituting (14) into (6). They are given by

$$C_{mn} = \frac{8b\sigma}{mn\pi^2\Delta_{mn}}\left\{\sigma + i\left[(m\pi)^2 + \left(\frac{n\pi}{b}\right)^2\right]\right\},$$

$$\text{for } m = 1,3,5,\ldots,\ n = 2,4,6,\ldots, \qquad (15)$$

$$C_{mn} = 0, \quad \text{otherwise},$$

where we define

$$\Delta_{mn} \equiv \left[(m\pi)^2 + \left(\frac{n\pi}{b}\right)^2\right]^2 + \sigma^2. \qquad (16)$$

Following a similar procedure as in deriving the damping torque in terms of the Fourier series solution, we obtain

$$T_d = -\frac{16 l_M w_M^3 p_a}{\pi^4 h_0}\left\{\theta \sum_{odd\,m}\sum_{even\,n}\frac{\sigma^2}{m^2 n^2 \Delta_{mn}} + \frac{1}{\omega}\dot{\theta}\sum_{odd\,m}\sum_{even\,n}\frac{\sigma}{m^2 n^2 \Delta_{mn}}\left[(m\pi)^2 + \left(\frac{n\pi}{b}\right)^2\right]\right\}. \qquad (17)$$

Now that we have successfully developed an analytical method for the squeeze film damping analysis using the series solution strategy, let us conclude this section by pointing out that the series solution strategy is a very common technique used to solve a general boundary value problem. The idea of using this strategy in our study maybe useful for many other applications.

VERIFICATION OF THE ANALYTICAL DAMPING MODEL

To examine the performance of the developed analytical damping model, we compare the analytical damping model with the numerical damping model. By the numerical damping model, we mean the damping torque determined by solving the nonlinear isothermal Reynold's equation using the implicit finite difference method [12,13]. Moreover, we compare the modeling results with the experimental measurements.

To illustrate, we here present figures with modeling results and/or experimental results for a prototype device. The parameters of this device are:

$$l_M = 1{,}500\mu m,\ w_M = 1{,}400\mu m,\ h_0 = 42\mu m,$$

$$f_n = 1.44 kHz,\ K = 4.49\times10^{-7}\ N.m/rad,$$

$$I = 5.51\times10^{-15}\ kg.m^2.$$

Here I is the moment of inertia of the mirror, K is the torsional stiffness of the torsion rods, and f_n denotes the first natural frequency of the system.

Figure 2 shows the time response of the angular displacement of the mirror under a resonant frequency ($f = 1.44\,kHz$) harmonic excitation. Among the three curves shown in this figure, the solid line curve denotes the external driving torque, the dashed line is obtained based on the analytical damping model in terms of the Fourier series solution, and the dot-dashed line is obtained based on the numerical damping model. The result corresponding to the double sine series damping model is not shown in Figure 2. This is because we have found that the Fourier series solution and the double sine series solution yield almost identical results for the dynamic response of the device. Therefore, we only show the results associated with the Fourier series solution.

We see from Figure 2 that the analytical damping model matches well with the numerical damping model. Even when the mirror is excited at its resonant frequency, we can only observe a small difference at the peak of the response curves.

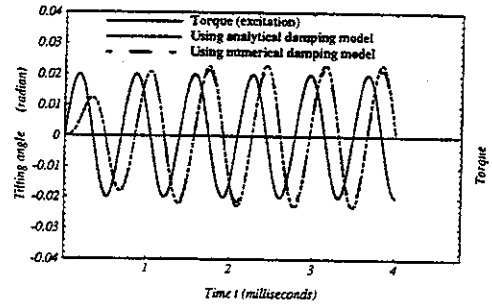

Figure 2. Time response of the mirror at resonant frequency harmonic excitation.

Figure 3 shows the frequency response function (of displacement) of the mirror. Here we compare the modeling results with the experimental results.

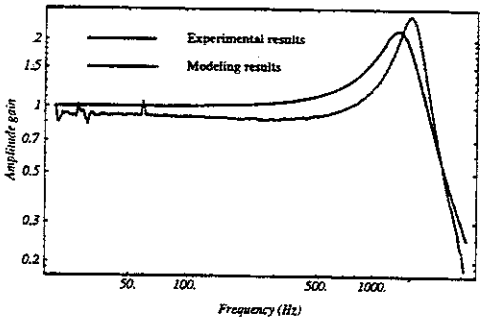

Figure 3. Frequency response function of the mirror.

From the modeling results, we see that due to the damping effect, the maximum response occurs at $f_m = 1.36kHz$, a little less than the resonant frequency. The quality factor of the torsion mirror is $Q = 2.20$. The damping ratio $\xi = 0.22$. Since $\xi < 1$, the system is underdamped.

From the experimental measurement results, the maximum response occurs at $f_m = 1.59kHz$, the quality factor is $Q = 2.58$, and the damping ratio $\xi = \frac{1}{2Q} = 0.19$. These are close to the modeling results obtained through the use of the analytical damping model.

ADVANCED INVESTIGATIONS

As mentioned before, the squeeze film damping force includes contributions from both the air spring effect and the dissipative damping effect. However, modeling results show that the air spring effect is negligible in our analysis. This is consistent with the results found by Langlois [1] and Starr [5], since the squeeze number σ is a very small value in the range of interest of our study. Therefore, in what follows, we drop the terms due to the air spring effect in the analytical formulae of the damping torque. This leads to a number of new observations. We shall discuss these observations using the double sine series solution which is more convenient for qualitative analysis. In addition, at the end of this section, we present a one term approximate formula for the squeeze film damping torque based on a convergence study of the series solutions.

Sensitivity of the Damping Torque to Changes in the Ambient Pressure

After dropping the terms due to the air spring effect, and recalling that $\sigma = \frac{12\mu\omega {l_M}^2}{p_a {h_0}^2}$, we obtain from (17) the following expression for the damping torque:

$$T_d = -\frac{192\mu {l_M}^3 {w_M}^3}{\pi^4 {h_0}^3}\dot{\theta} \sum_{\substack{odd\ m \\ even\ n}} \frac{(m\pi)^2 + \left(\frac{n\pi}{b}\right)^2}{m^2 n^2 \Delta_{mn}}. \qquad (18)$$

It is seen from (18) that the damping torque does not depend explicitly on the ambient pressure, but on the air viscosity μ and the squeeze number σ which both depend on the ambient pressure. For small σ, since T_d is a linear function of μ, and μ is not sensitive to changes in the ambient pressure, we conclude that the damping torque is not very sensitive to changes in the ambient pressure. This conclusion is supported by our experimental observations. It should be pointed out, however, that the above discussion is for ambient pressure greater than a certain value. As the pressure decreases and becomes smaller than that critical value, the damping behavior changes because of the slip flow condition [5,14]. The mean free path of the molecules increases as the pressure decreases. According to Starr [5], when the mean free path of the gas molecules within the film is about 1% of the film thickness, the

slip flow phenomenon occurs. We shall not discuss this subject further in the present paper.

Extension of the Analytical Damping Model

Although our analytical damping model is derived based on the harmonic dynamic response assumption, we show here that this damping model is still valid for the case of non-harmonic response. We see from (18) and (16) that the dependence of the damping torque on the harmonic response frequency ω is negligible. This is because the only parameter in (18) which depends on ω is the squeeze number σ which is related to Δ_{mn}, as shown in (16). However, for a reason similar to that mentioned previously, the effect of a change in σ (as a result of a change in ω) on the damping torque is negligible. On the other hand, for the case in which the angular displacement is a general function of time, we can imagine that this function is a combination of many harmonic functions of time (e.g., we can expand this time response function into a Fourier sine series over a certain range of time). Since for the linearized Reynold's equation, the principle of superposition works, we thus can combine the damping torque components contributed by different harmonic response functions, and get a formula which is the same as (18), with the exception of the physical meaning of the frequency parameter ω used in evaluating the squeeze number σ. In the case of harmonic response, ω is the harmonic response frequency, but in the case of non-harmonic response, it is a typical frequency of the squeeze film components. Therefore, we have shown that when the air spring effect is neglected, the analytical damping model is valid even if the dynamic response of the mirror is an arbitrary function of time. This result is important, since in general, even under harmonic excitation, the transient response of a device is not harmonic. However, this transient response is an essential aspect of the mirror's behavior that must be determined in our design process.

As an illustration, Figure 4 shows the modeling results of the time response of the mirror to a step load excitation. Both the result based on the analytical damping model and that based on the numerical damping model are shown in the figure. We see that the two sets of results match very well. Figure 5 shows the experimental results for the time response of the mirror to a rectangular wave excitation. The damping ratio ξ obtained from Figure 4 is equal to 0.22, and that from Figure 5 is equal to 0.19. These results are consistent with the results determined from the frequency response function (Figure 3).

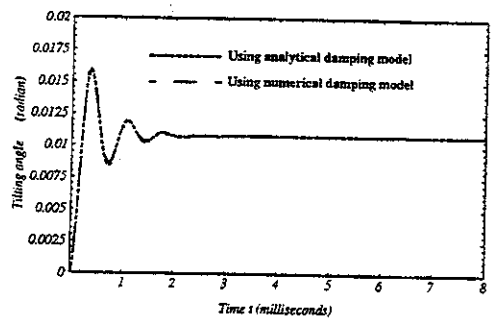

Figure 4. Time response of the mirror to a step load excitation.

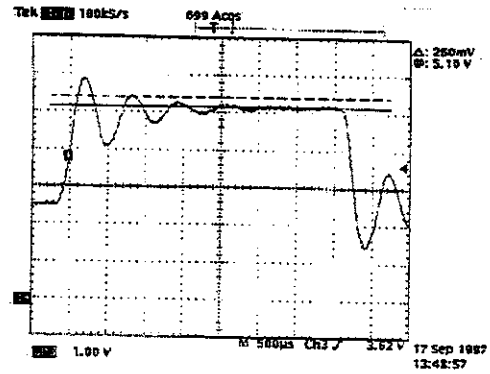

Figure 5. Experimental results for the time response of the mirror to a rectangular wave excitation.

The One Term Approximate Formula

From the numerical calculations, we find that both the series solutions for the squeeze film damping torque converge rapidly. Within the range of interest of our analysis, even the first term in each of the series solutions provides sufficient accuracy for the prediction of the damping torque. The Fourier series solution converges faster than the double sine series solution, and the first term of this solution provides a somewhat better approximation than that of the double sine series solution. However, the former has a much more complicated expression than the later. We thus prefer to present an approximate formula based on the first term of the double sine series solution. It is given by

$$T_d = -K_{rot}\frac{\mu l_M {w_M}^5}{{h_0}^3}\dot{\theta},$$
$$\text{where } K_{rot} \equiv \frac{48}{\pi^6(b^2+4)}. \quad (19)$$

This formula is very similar to the formula provided by [9]. However, there is a difference in the coefficient K_{rot} between equation (19) and the formula presented in [9].

CONCLUSION

We have developed an analytical method for the squeeze film damping effect on the dynamic response of a MEMS torsion mirror. This analytical method has been verified by comparing the analytical damping model with the numerical damping model, and by comparing the modeling results with the experimental measurement results for a prototype device. Having been developed under the harmonic response assumption, the analytical method is finally extended to the case of nonharmonic response. The significance of this analysis is that it saves a great amount of computation time required for numerically solving the nonlinear isothermal Reynold's equation.

ACKNOWLEDGEMENTS

The authors of this paper would like to thank Professor S. D. Senturia in MIT for discussing the Reynold's equation, Bob Lofthus in Xerox WCR&T for providing experimental data, Gregory Zack in Xerox DRI for discussing the double sine series solution, and Michael Cavanaugh in Xerox DRI and Frank Adelstein in Cornell University for their help with the computational aspects of this research.

REFERENCES

[1] W. E. Langlois, Isothermal squeeze films, Quarterly Applied Mathematics, Vol. XX, No. 2, 1962, pp. 131-150.

[2] F. Pan, J. Kubby, E. Peeters, O. Vitomirov, D. Taylor, S. Mukherjee, Design, modeling and verification of MEMS silicon torsion mirror for applications in xerography, SPIE conference, September 1997.

[3] H. G. Elrod, A derivation of the basic equations for hydrodynamic lubrication with a fluid having constant properties, Quarterly of Applied Mathematics, 17, pp. 349-359, 1960.

[4] J. J. Blech, On isothermal squeeze films, Journal of Lubrication Technology, Oct. 1983, Vol. 105, pp. 615-620.

[5] J. B. Starr, Squeeze film damping in solid-state accelerometers, Tech. Digest, IEEE Solid State Sensor and Actuator Workshop, Hilton Head Island, SC, June 1990, pp. 44-47.

[6] M. Andrews, I. Harris, and G. Turner, A comparison of squeeze film theory with measurements on a microstructure, Sensors and Actuators A, 36, 1993, pp. 79-87.

[7] Y. J. Yang and S. D. Senturia, Numerical simulation of compressible squeeze film damping, Tech. Digest, IEEE Solid State Sensor and Actuator Workshop, Hilton Head Island, SC, June 1996, pp. 76-79.

[8] R. B. Darling, C. Hivick, and J. Xu, Compact analytical models for squeeze film damping with arbitrary venting conditions, Transducers 97, 1997 International Conference on Solid-State Sensors and Actuators, Vol. 2, pp. 1113-1116.

[9] W. *Dötzel*, T. Gessner, R. Hahn, . Kaufmann, K. Kehr, S. Kurth, J. Mehner, Silicon mirrors and micro-mirror arrays for spatial laser beam modulation, Transducers 97, 1997 International Conference on Solid-State Sensors and Actuators, Vol. 1, pp. 81-84.

[10] W. S. Griffin, H. H. Richardson, and S. Yamanami, A study of squeeze film damping, ASME Journal of Basic Engineering, June 1996, pp. 451-456.

[11] F. Pan, J. Kubby, E. Peeters, A. Tran, and S. Mukherjee, Squeeze film damping effect on the dynamic response of a MEMS torsion mirror, submitted to Journal of Micromechanics and Microengineering.

[12] W. A., Michael, Approximate solution of time-dependent gas film lubrication problems, IBM Research Report, RJ-205, 1961b.

[13] A. Bellman, Dynamic Programming and Partial Differential Equations, Academic Press, New York and London, 1972.

[14] T. Veijola, H. Kuisma, J. *Lahdenpeä*, T. *Ryhänen*, Equivalent-circuit model of the squeeze film in a silicon accelerometers, Sensors and Actuators A, 48, pp. 239-248, 1995.